Journal of Global Change Data & Discovery. 2022, 6(4): 607-618
www.geodoi.ac.cn

Methods and Results of Identifying a Road Material Dataset from GF–6 Remote Sensing Data in the Langfang Area

Cui, Y. P.

China Highway Engineering Consulting Group Co., Ltd., Beijing 100097

Abstract: Based on high-resolution remote sensing techniques, the spectral characteristics of different road materials are compared, and a road material recognition experimental dataset is developed using machine learning technology. The experimental dataset consists of three parts: (1) a remote sensing image dataset, including GF-6 WFV and GF-2 data; (2) a spectral characteristic index dataset, including a spectral difference index dataset, spectral ratio index dataset, spectral variance index dataset and a spectral normalization index dataset; (3) a sample dataset which includes collected road material type samples based on Google Image and Baidu street view data. In the road material recognition result dataset, the road material recognition accuracy reaches 80.07%, and the kappa coefficient is 0.70, reaching acceptable accuracy requirements.

Keywords: Road material; Machine learning; High-resolution remote sensing

DOI: https://doi.org/10.3974/geodp.2022.04.12

CSTR: https://cstr.escience.org.cn/CSTR:20146.14.2022.04.12

Dataset Availability Statement:

The dataset supporting this paper was published and is accessible through the *Digital Journal of Global Change Data Repository* at: https://doi.org/10.3974/geodb.2022.08.10.V1 or https://cstr.escience.org.cn/CSTR:20146.11.2022.08.10.V1.

1 Introduction

Under the strategical guidance of a country with a strong transportation sector, China has vigorously promoted the development of transportation and accelerated the formation of a comprehensive three-dimensional transportation network. Under the current situation of rapid development of transportation, the traditional means of technology can no longer meet the current needs[1]. Information technology represents an effective means to meet the intelligent and scientific decision-making and management needs of the transportation industry. Improving the digitalization of the transportation industry is also an important way

Received: 08-10-2022; **Accepted:** 07-12-2022; **Published:** 24-12-2022

Foundations: GF-6 (07-Y30B03-9001-19/21, 87-Y50G28-9001-22/23)

Author Information: Cui, Y. P. EVU-6053-2022, China Highway Engineering Consulting Group Co., Ltd., songzl0906@163.com

Data Citation: [1] Cui, Y. P. Methods and results of identifying a road material dataset from GF-6 remote sensing data in the Langfang area [J]. *Journal of Global Change Data & Discovery*, 2022, 6(4): 607–618. https://doi.org/10.3974/geodp.2022.04.12. https://cstr.escience.org.cn/CSTR:20146.14.2022.04.12.

[2] Cui, Y. P. Experimental dataset of identifying road material using GF-6 images [J/DB/OL]. *Digital Journal of Global Change Data Repository*, 2022. https://doi.org/10.3974/geodb.2022.08.10.V1. https://cstr.escience.org.cn/CSTR:20146.11.2022.08.10.V1.

to develop transportation in the new era.

The rapid development of high-definition remote sensing technology and its increasingly prominent technical advantages have led to the rapid expansion and deepening of its applications worldwide, with increasingly obvious application benefits. Currently, remote sensing technology is widely used in many fields, such as agriculture, forestry, geology, geography, oceanography, hydrology, meteorology, mapping, environmental protection, and military reconnaissance. Under the wave of digitalization sweeping the world, the "Outline of Planning for National Comprehensive Three-Dimensional Transportation Network" issued by the Central Committee and the State Council has even proposed "promoting the application of satellite communication technology, new generation communication technology, high-definition remote sensing satellite and artificial intelligence in the industry". High-definition remote sensing technology provides an opportunity for the digital transformation of the transport industry. Because of its advantages of high timeliness, wide coverage, and high spatial resolution, high-definition remote sensing has become an important means of dynamic information collection in the transport industry, playing an important role in the whole life cycle of transport planning, survey, construction, operation, maintenance, disaster prevention and mitigation, and providing technical support to improve the level of information associated with the transport industry. It has played an important role in the whole life cycle of transport planning, survey, construction, operation, maintenance, disaster prevention, and mitigation, and has also provided technical support to improve the level of information technology in the transport industry[2].

As the most common and widely used mode of transportation[3], road analysis is important for grasping the different road compositions and distribution in a region. Currently, the types of road surfaces in China are mainly divided into asphalt concrete pavement, cement concrete pavement, asphalt through pavement (or asphalt gravel pavement), gravel pavement, cement gravel pavement, and earth pavement. Different road surface materials, such as asphalt, cement, and dirt, reflect different spectral information. Road surface materials can be identified and differentiated based on the differences in the spectral, texture, direction, and brightness information of different road materials on the remote sensing images. At present, many scholars have carried out relevant research work in the remote sensing extraction of road pavement materials.

Mintzer *et al*. have used remote sensing to detect tarmac conditions and provide data to support research into urban traffic patterns[4]. Gardner *et al*. acquired remote sensing images taken by an airborne visible/infrared imaging spectrometer in California to achieve the extraction of road surface materials in California[5], Grote *et al*. achieved the extraction of roads using high-precision aerial images, providing an accurate data source for updating the road database[6]. Suchand *et al*. extracted traffic roads by applying TerraSAR-X track interferometry[7]. Buslaev *et al.* achieved automatic extraction of road networks by investigating deep learning algorithms such as convolutional neural networks[8].

Domestic scholars have researched pavement materials using different types of remote sensing data, such as hyperspectral, multispectral, and LiDAR. She Yuchen *et al*. obtained hyperspectral data of different pavement materials, such as asphalt road, concrete, bare soil, and grass, using a ground feature spectrometer, and calculated the spectral mean, first-order differentiation, second-order differentiation and logarithm after inversion. They compared and analyzed the spectral characteristic curves of four different materials and concluded that taking the logarithm after inversion was the most effective method for identifying the type of road pavement materials[9]. Jin *et al*. used hyperspectral remote sensing to analyze the spectral reflection absorption characteristics of pavements in different spectral bands and studied the spectral response change pattern of asphalt pavements during the aging process to determine the aging degree of pavements[10]. Lu, *et al*. obtained field observations of

hyperspectral data of typical roads such as cement concrete roads, asphalt roads, brick roads, and dirt roads to study the best waveband to distinguish between different road types[11]. Zhang *et al*. applied the combination of multispectral and hyperspectral to identify road surface materials[12]. They proceeded to identify the road surface materials of the Beijing-Chengdu Expressway based on the hyperspectral image of Gaoxin-1, combined with the hyperspectral data measured in the field[12]. In extracting the pavement material with high-resolution images, Gao *et al*. avoided the influence of building shadows and low vegetation groups by using airborne LiDAR data[13].

The structural elements of the road surface are important factors for interpreting the road grade and are of great significance for grasping the composition and distribution of different roads in the region[14]. With the construction and development of "four good rural roads", "precise poverty alleviation", and the three-year action plan for poverty alleviation in transportation, the extraction of road surface types has become an indispensable step[15]. Timely, objective, accurate, and comprehensive data on rural road surface structural elements can be used to provide objective data support for road planning, which is of great significance. Using the new spectral information of the yellow-light band of the Gaofen-6 satellite and the high-resolution characteristics of the Gaofen-2 satellite, different material compositions of rural road surfaces (such as dirt roads) can be identified, forming a complete dataset that can be used in the identification and collection of road surface information. This study develops a method for producing road material identification datasets based on the characteristics of the HRS technology and validates the accuracy of the results to form a complete set of datasets to support road planning.

2 Metadata of the Dataset

The metadata of the Experimental dataset of identifying road material using GF-6 images[16] is summarized in Table 1. It includes the dataset full name, short name, authors, year of the dataset, temporal resolution, spatial resolution, data format, data size, data files, data publisher, and data sharing policy, etc.

3 Data Sources and Production

The remote sensing data include GF-6 WFV data, GF-2 data, Google images, and Baidu Street view data. The GF-6 WFV and GF-2 data were obtained from the China Resources Satellite Application Centre[18] and mainly used for the identification of road surface material types. Google images and Baidu Street View data were used to collect road material type samples. The satellite parameters of GF-6 and GF-2 data are shown in Table 2.

3.1 Remote Sensing Image Pre-processing

When imaging remote sensing images, there is a certain amount of geometric distortion, atmospheric extinction, and distortion of radiation levels that occur for various reasons. These geometric and radiation-level distortions can affect the identification of road surface materials. The acquired HMS-2 and HMS-6 data are preliminary L1-level products and require pre-processing sessions to correct distortions, blurring, and noise generation during the image acquisition process. The pre-processing process includes geometric alignment, orthorectification, atmospheric correction, radiometric correction, etc. After pre-processing, the images can meet the needs of road material identification. The steps for pre-processing remote sensing images are already very mature technologies and will not be repeated in this paper.

3.2 Image Fusion Processing Based On Spectral Unmixing

In this paper, we use the data taken by the multi-spectral medium-resolution Wide Field

Table 1 Metadata summary of the Experimental dataset of identifying road material using GF-6 images

Items	Description
Dataset full name	Experimental dataset of identifying road material using GF-6 images
Dataset short name	GF_RoadMaterial
Author	Cui, Y. P. EVU-6053-2022, China Highway Engineering Consulting Group Co., Ltd., songzl0906@163.com
Geographical region	Langfang city, Hebei province
Year	2020
Spatial resolution	0.8 m
Data format	.dat, .shp, .xlsx, .tif
Data size	3.69 GB (1.62 GB after compression)
Dataset composition	Remote sensing image data, spectral feature index data, sample data, and road material identification result data
Foundations	GF-6 (07-Y30B03-9001-19/21, 87-Y50G28-9001-22/23)
Data publisher	Global Change Research Data Publishing & Repository, http://www.geodoi.ac.cn
Address	No. 11A, Datun Road, Chaoyang District, Beijing 100101, China
Data sharing policy	***Data*** from the Global Change Research Data Publishing & Repository includes metadata, datasets (in the *Digital Journal of Global Change Data Repository*), and publications (in the *Journal of Global Change Data & Discovery*). ***Data*** sharing policy includes: (1) ***Data*** are openly available and can be free downloaded via the Internet; (2) End users are encouraged to use ***Data*** subject to citation; (3) Users, who are by definition also value-added service providers, are welcome to redistribute ***Data*** subject to written permission from the GCdataPR Editorial Office and the issuance of a ***Data*** redistribution license; and (4) If ***Data*** are used to compile new datasets, the 'ten per cent principal' should be followed such that ***Data*** records utilized should not surpass 10% of the new dataset contents, while sources should be clearly noted in suitable places in the new dataset[17]
Communication and searchable system	DOI, CSTR, Crossref, DCI, CSCD, CNKI, SciEngine, WDS/ISC, GEOSS

Table 2 Parameters of GF-6 and GF-2 satellite

Satellite Parameters	GF-6				GF-2	
	High resolution cameras (PMS)		Wide format cameras (WFV)		High resolution cameras (PMS)	
Spectral range	Panchromatic	0.45–0.90 μm			Panchromatic	0.45–0.90 μm
	B1 (Blue Band)	0.45–0.52 μm	B1 (Blue Band)	0.45–0.52 μm	B1 (Blue Band)	0.45–0.52 μm
	B2 (Green Band)	0.52–0.60 μm	B2 (Green Band)	0.52–0.60 μm	B2 (Green Band)	0.52–0.59 μm
	B3 (Red Band)	0.63–0.69 μm	B3 (Red Band)	0.63–0.69 μm	B3 (Red Band)	0.63–0.69 μm
	B4 (Near Infrared)	0.76–0.90 μm	B4 (Near Infrared)	0.76–0.90 μm	B4 (Near Infrared)	0.77–0.89 μm
			B5 (Red edgeI)	0.69–0.73 μm		
			B6 (Red edgeII)	0.73–0.77 μm		
			B7 (Purple Band)	0.40–0.45 μm		
			B8 (Yellow Band)	0.59–0.63 μm		
Resolution	Panchromatic	2 m	Panchromatic	/	Panchromatic	1 m
	Multispectral	8 m	Multispectral	≤16 m	Multispectral	4 m
Width	≥90 km		≥800 km		45 km	

Camera (WFV) with a resolution of 16 m for the HMS-6 remote sensing satellite data and a spatial resolution of 0.8 m for the HMS-2 remote sensing satellite image data. As the roads are linear in length, this paper uses the spectral unmixing method to fuse the HMS-6 and HMS-2 images, which improves the spatial resolution of the images while retaining the features of the eight bands of HMS-6. The basic principle of image fusion by spectral unmixing is described by the following method: first, the GF-6 multi-spectral data and the high-resolution GF-2 panchromatic data are unmixed to obtain the multispectral image

spectral basis matrix, then the multi-spectral image spatial coefficient matrix, the panchromatic image spectral basis matrix, and the panchromatic image coefficient matrix, and then the 1-m resolution 8-band image is obtained by multiplying the optimally solved multi-spectral image spectral basis matrix with the panchromatic image coefficient matrix. The fused data were obtained by multiplying the optimally solved multi-spectral image spectral basis matrix with the panchromatic image coefficient matrix. In this paper, we refer to the spectral unmixing method of Zhang *et al*.[19] and do not repeat the detailed procedure.

4 Method of Producing Road Material Datasets

4.1 Study Area

An area in the eastern part of Langfang city was chosen as the test bed for the study area (Figure 1), which has a full range of traffic road types and basically has complete coverage by Baidu Street View data. Langfang is located in the central-eastern part of Hebei province, bordering Beijing to the north, Tianjin to the east, Cangzhou to the south, and Baoding to the west, with a total area of 6,429 km^2. Langfang is located in the core hinterland of the "Golden Triangle" of Beijing, Tianjin, and Xiong'an New Area, and is an important node city in the world-class city cluster with Beijing as the core. By the end of 2021, Langfang had 857 km of national roads, 497 km of provincial roads, 778 km of county roads, 1,793 km of township roads, 42 km of special roads, and 7,489 km of village roads. The total mileage of roads in the city is 11,460,000 km, and the road density is 178 km/100 km^2, ranking first in the province.

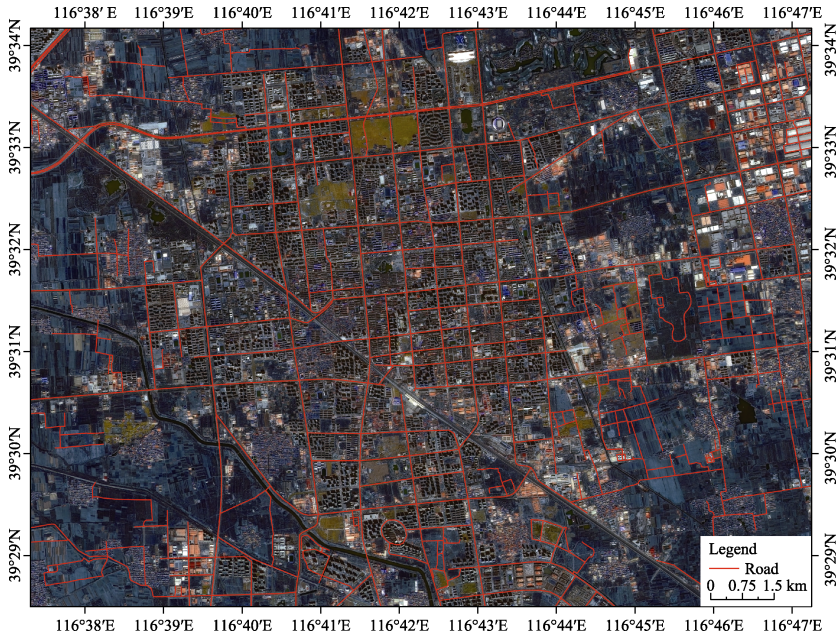

Figure 1 Maps of location of the experimental area

4.2 Technical Routes

The BP neural network regression is used to predict the importance of each index band on the identification of road surface material type, and the SVM classification filters the best combination of bands. This approach is based on GF-6 WFV data and GF-2 data fusion to obtain high-resolution data containing eight bands, combined with the calculated four road

spectral indices and first-order spectral derivatives using the road-material type sample dataset obtained from Baidu Street View. In this way, the road surface material types were identified as illustrated by the technical route shown in Figure 2.

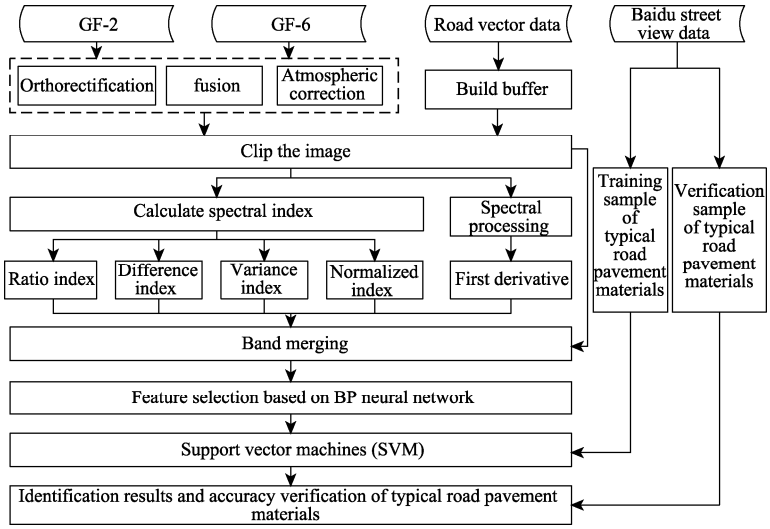

Figure 2 Technical flowchart of dataset development

4.3 Principles of Road Material Dataset Production

4.3.1 Spectral Characteristic Index Calculation

According to previous research, the spectral feature index of pavement is involved in the pavement material identification as a band, which can enhance the spectral characteristics of roads with different material types[20] and help improve the accuracy of identification results. In this paper, different spectral feature indices are constructed using the operation of the near-infrared band and blue light band, and the difference between their reflectances can serve as a basis to construct the spectral difference index (Equation 1), the ratio of the reflectance of the two constructs the spectral ratio index (Equation 2), the variance of the ratio of the reflectance of the two constructs the spectral variance index (Equation 3), and the normalized value of the reflectance of the two constructs the spectral normalized index (Equation 4).

$$SDI = NIR - Blue \tag{1}$$

$$SRI = \frac{Blue}{NIR} \tag{2}$$

$$SVI = Variance\left(\frac{Blue}{NIR}\right) \tag{3}$$

$$SNI = \frac{NIR - Blue}{NIR + Blue} \tag{4}$$

4.3.2 Optimal Waveband Selection Based on BP Neural Networks

After obtaining the spectral feature indices, the first-order derivatives of each band in the original image were calculated, and a total of 20 bands of data were obtained by band merging with eight bands of the remote sensing image. The samples of asphalt roads, concrete roads, and dirt roads are selected from Baidu Street View by visual inspection, and then the spectral feature information of the samples is obtained from the merged image data.

To improve the accuracy of road material recognition, it is necessary to rank the importance of numerous bands and select the best band to distinguish road material recognition. In this paper, the BP neural network (Back-ProPagation Network) can be used for data prediction and classification[20], is applied to select the best band. The wavebands with relatively high contributions can be included in the best combination of wavebands for road material identification.

4.3.3 Support Vector Machines

After the optimal band selection was completed for the images, the images were classified according to the samples of different materials to obtain classification results for asphalt roads, concrete roads, and dirt roads. The classification method chosen in this paper uses a Support Vector Machine (SVM), which was first proposed by Cortes and Vapnik in 1995 and is a binary classification model with obvious advantages in solving small sample and non-linear recognition problems; therefore, an SVM has obvious superiority in remote sensing image classification. This paper uses the SVM method to achieve fast recognition of road materials.

4.3.4 Identification of Road Surface Material Types

The SVM approach to remote sensing image classification is oriented towards the pixel level and the classification results obtained are also in the form of pixel levels. Therefore, there is fragmentation in the results of SVM-based road material recognition. In general, a road consists of the same material, and the fragmentation problem can be solved by the plural. First, this paper constructs a buffer (three pixels) of the road based on the road centerline vector data with the intent of avoiding the influence of other features. The plural of the statistical pavement type is counted for the identification result; for example, the plural of a road is the attribute value indicating asphalt road, which means that the road is an asphalt road, and the statistical plural is the attribute value of the pavement type of the road.

4.4 Dataset Accuracy Validation Methods

Accuracy verification refers to the comparison of the results of remote sensing image recognition with the actual results to determine the accuracy of the recognition process. The common accuracy evaluation method is the confusion matrix (also known as error matrix), which calculates the recognition accuracy in the form of an n-row and n-column matrix, which mainly include: precision, recall, overall accuracy, and the kappa coefficient.

The relationship between the hypothetical identification results and the true results is shown in Table 3.

Table 3 Hypothetical relationship between identification results and real results

Hypothetical relationship	Forecast-positive example	Forecast-negative example
Real-positive example	TP-true example	FN-false counterexample
Real-counter examples	FP-false positive example	TN-true counterexample

(1) Precision: the number of correctly classified positive samples as a proportion of the number of all positive samples classified by the classifier.

$$P = \frac{TP}{TP + FP} \tag{5}$$

(2) Recall: the number of correctly classified positive samples as a proportion of the number of all positive samples classified by the classifier.

$$R = \frac{TP}{TP + FN} \tag{6}$$

(3) Overall Accuracy: the number of correctly classified samples as a proportion of the number of all samples.

$$OA = \frac{TP + TN}{TP + FN + FP + TN} \tag{7}$$

4) Kappa coefficient: indicates the proportion of the evaluated classification that produces fewer errors than a completely random classification.

$$Kappa = \frac{N\sum_{i=1}^{r} x_{ii} - \sum_{i=1}^{r}(x_{i+} \times x_{+i})}{N^2 - \sum_{i=1}^{r}(x_{i+} \times x_{+i})} \tag{8}$$

where *TP* denotes positive samples correctly classified by the model; *FN* denotes positive samples incorrectly classified by the model; *FP* denotes negative samples incorrectly classified by the model; TN denotes negative samples correctly classified by the model; N denotes the total number of samples; x_{ii} denotes the values in row *i* and column *i* (main diagonal); *r* denotes the number of rows in the error matrix; x_{i+} and x_{+i} denote the sum of row *i* and column *i*, respectively.

5 Data Results and Validation

5.1 Dataset Composition

The dataset consists of four folders.

(1) Remote sensing image dataset: including the GF-6 Wide Format (WFV) and GF-2 remote sensing image data for the study area.

(2) Spectral feature index dataset: including the spectral difference index dataset, spectral ratio index dataset, spectral variance index dataset, and spectral normalized index dataset.

(3) Sample dataset: based on Google images and Baidu Street View data to collect samples of road material types.

(4) Road material recognition result dataset.

5.2 Data Results

(1) Data Fusion Results

The GF-6 WFV data has a resolution of better than 16 m, which is relatively coarse and cannot be directly used for road surface type identification. The experiment fused the GF-6 WFV data with the contemporaneous GF-2 data by the GS fusion method (Definition needed) to obtain high-resolution fused data (as shown in Figure 3). Before fusion, the GF-6 WFV and GF-2 data were pre-processed with radiometric correction, atmospheric correction, and orthorectification correction to remove the influence of the atmosphere and cloud interference so that the fused data could effectively indicate the reflectance of the surface. The fused data consists of eight bands with a resolution of 1 m. This ensures the high spatial resolution of the data but also adds two red-edge bands, a violet band, and a yellow band, which allows the recognition of road surface materials with clear road texture and good visual effects.

(2) Spectral index results

The spectral index formula was used to obtain spectral feature maps for the spectral difference index, spectral ratio index, spectral variance index, and spectral normalization index (Figure 4). The four types of spectral index feature maps are calculated based on the blue and near-infrared bands to enhance the spectral characteristics of different material types of roads, while the index calculation eliminates the variation in the images themselves and systematic errors. The addition of spectral indices can complement the spectral features

of the original data and improve the accuracy of road surface type identification. It is important to note that in the calculation of the ratio index, there are cases where the inverse color ratio in the NIR band is 0. In this case, the ratio index is set to a special value of 9,999 for the region where this condition is met.

(a) Image before fusion (b) Image after fusion

Figure 3 GF-6 WFV satellite images before and after fusion

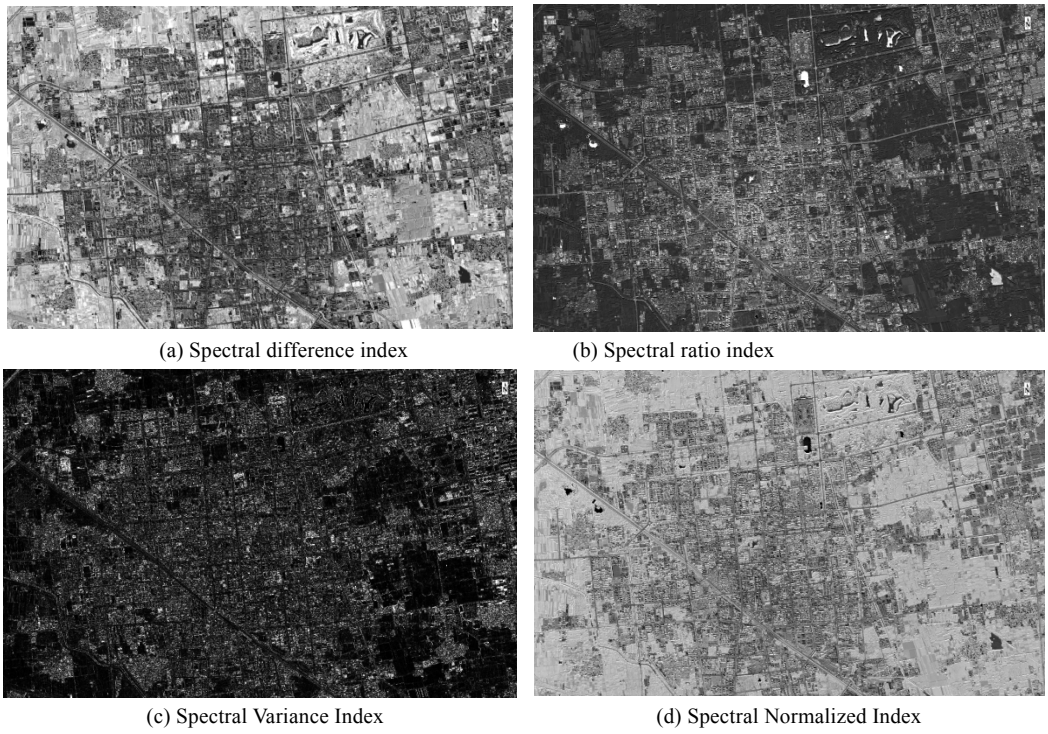

(a) Spectral difference index (b) Spectral ratio index

(c) Spectral Variance Index (d) Spectral Normalized Index

Figure 4 The spectral indexes of road material

(3) Band feature selection

The experiments used the BP neural network model, combined with the acquired road pavement type sample data, to establish a band importance (contribution) model that can easily distinguish between pavement material types. The model results are shown in Figure 5. As can be seen from the figure, there are a total of 20 bands involved in the whole model, of which 8 bands consist of the original data, 4 bands of the spectral index and 8 bands of the first-order derivatives of the original data (where Red_deriv represents the red band derivatives, NIR_deriv represents the NIR band derivatives, SNI represents the normalized

spectral index, SRI represents the ratio spectral index, Red_edge2 _deriv stands for the red edge II band derivative, NIR stands for the near-infrared band, Red_edge1_deriv stands for red edge I band derivative, Red_edge2 stands for red edge II band, Red stands for the red band, Purple stands for the purple band, Red_edge1 stands for the red edge I band, Blue stands for the blue band, Yellow stands for the yellow band, Blue_deriv for the blue band derivative, Yellow_deriv for the yellow band derivative, Green for the green band, Purple_deriv for the purple band derivative, Var for the variance spectral index, Green_deriv for the green band derivative, and SDI for difference spectral index). The bands were ranked according to the importance of participation, and the top six accounted for more than 5% of feature importance. The accuracy of the model was calculated by adding the bands one by one according to feature importance, and it was found that the accuracy of the model was highest when the eight band was added, so the experiment used the top eight bands with larger importance values for road pavement type identification, which include: the red band derivative, near-infrared band derivative, normalized spectral index, the ratio spectral index, the red edge II band derivative, the NIR representing the NIR band, the derivative of the red edge I band, and the red edge II band.

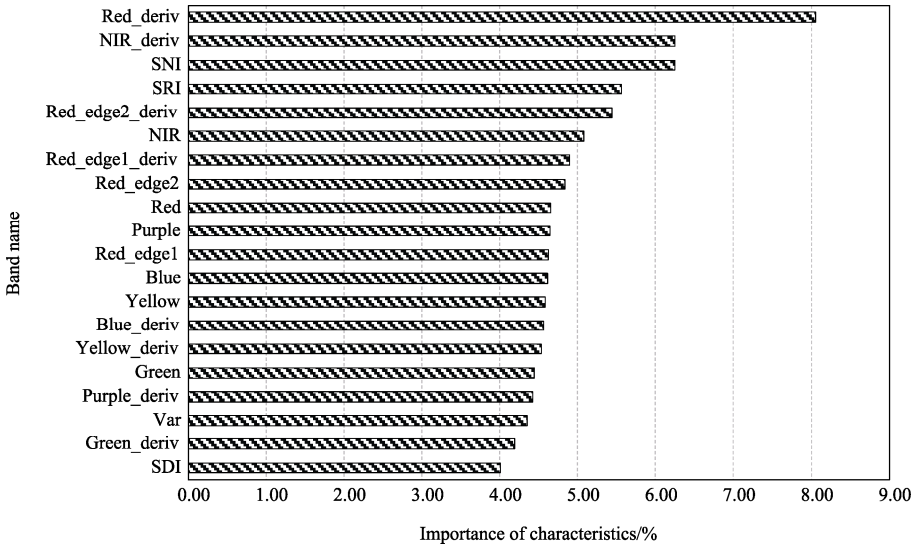

Figure 5 Importance of band features in BP neural network model

(4) Identification results

To improve the recognition accuracy of road-pavement types, a road buffer zone (5 m) is established based on the road centerline, and the interference of features outside the buffer zone is excluded, allowing for the recognition of road-pavement material types to be carried out only within the road buffer zone. Based on the visually acquired sample data of concrete roads, asphalt roads, and dirt roads, the SVM method is facilitated to identify the road-pavement types. The road-pavement type extraction results and the actual results are shown in Figure 6. In the study area, the asphalt road pavement is wider and has the best extraction results with stronger road connectivity; the concrete and dirt road pavements are narrower, and the extracted pavement type connectivity is weaker, and the surrounding features will also have some influence on the road-pavement type identification.

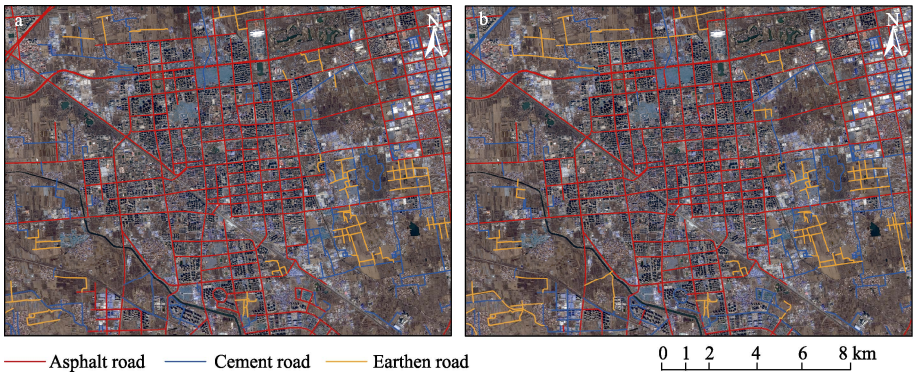

(a) Real results (b) Recognition results

Figure 6 Comparison images of road material between recognition results and real results

5.3 Data Validation Applications

In the results of road-pavement material identification based on GF-6 WFV and GF-2 fusion data, a total of 271 roads were selected in the study area, and information on each road-pavement material type was obtained through visual interpretation, i.e., pavement material type verification samples. A confusion matrix was used to validate the experimental results, as shown in Table 4. The overall accuracy of the road-pavement material type recognition results was 80.07%, with a kappa coefficient of 0.70. In terms of overall road-pavement recognition accuracy, the highest accuracy rate (92.65%) was achieved for asphalt road-pavement type recognition, and the lowest accuracy rate (75.00%) was achieved for cement road-pavement type recognition; the highest recall rate (79.65%) was achieved for cement road-pavement type recognition, and the lowest recall rate (75.00%) was achieved for asphalt road-pavement type identification. The overall road-pavement type identification results are more accurate, the precision meets certain requirements, and the method can be used for a wide range of road-pavement material type identification work.

Table 4 The results of precision validation

Roads (stripes)		Identification results				Recall rate (R)
		Asphalt roads	Concrete roads	Dirt roads	Total	
Actual results	Asphalt roads	63	20	1	84	75.00%
	Concrete roads	5	90	18	113	79.65%
	Dirt roads	0	10	64	74	77.11%
	Total	68	120	83	271	
Accuracy (P)		92.65%	75.00%	86.49%		
Overall accuracy OA = 80.07%						
Kappa factor: 0.70						

6 Discussion and Conclusion

Based on GF-6 WFV and GF-2 data, a high-resolution dataset (0.8 m resolution) was obtained by fusing the data using a GS algorithm. In this way, the spectral difference index, ratio index, variance index, normalized index, and the first-order derivative of the image were calculated. The sample dataset of road-pavement material types were visually interpreted by applying Baidu Street View data, and the importance of band features was predicted by BP neural network. The optimal band combination was selected, and the SVM

method was used to recognize road-pavement material types. We arrived at the following conclusions.

(1) The fused data has multi-band characteristics and high spatial resolution, which meets the recognition of road-pavement types.

(2) The best waveband combinations based on the BP neural network are the red band derivative, NIR band derivative, normalized spectral index, ratio spectral index, red edge II band derivative, NIR representing the NIR band, derivative of red edge Ⅰ band, and the red edge Ⅱ band, for a total of eight bands.

(3) The overall recognition accuracy of road pavement material is 80.07%, and the kappa coefficient is 0.70. The dataset meets acceptable accuracy requirements.

Conflicts of Interest

The authors declare no conflicts of interest.

References

[1] Zhang, L. Modern transportation information network and communication technology [M]. Shanghai: Tongji University Press, 2007.

[2] Manzo, C., Mei, A., Salvatori, R., *et al*. Spectral modeling used to identify the aggregates index of asphalted surfaces and sensitivity analysis [J]. *Construction & Building Materials*, 2014, 61: 147–155.

[3] Fu, C. Opportunities and challenges of highway survey and design in the era of big data [D]. Xi'an: Chang'an University, 2016.

[4] Minter, O. W. Manual of remote sensing second interpretations and applications [S]. American society of photogrammetry, Falls Church, VA, 1983, 2: 1955–2109

[5] Gardner, M., Roberts, D. A., Funk, C., *et al*. Road extraction from AVIRIS using spectral mixture and Q-tree filter techniques [C]. Technical Report, May, 2001. University of California, Santa Barbara, National Consortium on Remote Sensing and Transportation: Infrastructure, 2001.

[6] Grote, A., Heipke, C. Road extraction for update of road databases in suburban areas [J]. *Remote Sensing and Spatial Information Science*, 2008, XXXVII-B3b: 563–568.

[7] Suchandt, S., Runge, H., Breit, H., *et al.* Automatic Extraction of Traffic Flows Using TerraSAR-X Along-Track Interferometry [J]. *IEEE Transactions on Geoscience & Remote Sensing*, 2010, 48(2): 807–819.

[8] Buslaev, A., Seferbekov, S., Iglovikov, V., *et al*. Fully convolutional network for automatic road extraction from satellite imagery [C]. Conference on Computer Vision and Pattern Recognition Workshops (CVPRW). IEEE, 2018.

[9] She, Y. C., Lin, F., Sun, H. Hyperspectral characterization of major road pavement materials [J]. *Journal of Central South University of Forestry Science and Technology*, 2014, 34(11): 120–139.

[10] Jin, X., Zhang, X. F., Luo, L., *et al*. A preliminary investigation on the spectral feature analysis of highway pavement and remote sensing monitoring method of asphalt pavement deterioration [J]. *Journal of Geoinformation Scienc*e, 2017, 19(5): 672–681.

[11] Lu, P. P., Dai, J. G., Shi, X. Z. Analysis of spectral features of four typical roads based on hyperspectral remote sensing [J]. *Mapping and Spatial Geographic Information*, 2019, 42(5): 141–144.

[12] Zhang, Y. X., Xu, W., Wang, Y., *et al*. Discriminative analysis of pavement materials based on spectral features [J]. *Journal of Changsha University of Technology* (*Natural Science Edition*), 2017, 14(4): 1–9.

[13] Gao, L. P. Research on road extraction based on airborne LiDAR and high-resolution remote sensing images [D]. Xuzhou: China University of Mining and Technology, 2014.

[14] Zhang, X. B., Cheng, R. S., Wang, L. J. Investigation and analysis of the current situation of asphalt pavement thickness of highways in China [J]. *Henan Transportation Science and Technology*, 1999(1): 3–5.

[15] Li, X. P. Make up for shortcomings to build "four good rural roads" [J]. *China Road*, 2017(17): 20–25.

[16] Cui, Y. P. Experimental dataset of identifying road material using GF-6 images [J/DB/OL]. *Digital Journal of Global Change Data Repository*, 2022. https://doi.org/10.3974/geodb.2022.08.10.V1. https://cstr.escience.org.cn/CSTR:20146.11.2022.08.10.V1.

[17] GCdataPR Editorial Office. GCdataPR data sharing policy [OL]. https://doi.org/10.3974/dp.policy.2014.05 (Updated 2017).

[18] China Resources Satellite Application Centre. http://www.cresda.com/CN/.

[19] Zhang, Y. L., Fu, Y. H., Ren, K., et al. Fine identification of road material by fusion of multi-source remote sensing data [J]. *Highway*, 2021, 66(3): 206–214.

[20] Xiao, G. F., Zhang, Y. L., Yang, X., *et al*. Identification of typical road pavement types based on GF-2 remote sensing images [J]. *Highway*, 2020, 65(10): 8.